Comprehensive two-dimensional gas chromatography coupled with time of flight mass spectrometry featuring tandem ionization: Challenges and opportunities for accurate fingerprinting studies

Comprehensive two-dimensional gas chromatography coupled with time of flight mass spectrometry featuring tandem ionization: challenges and opportunities for accurate fingerprinting studies

Chiara Cordero[1*] Alessandro Guglielmetti[1], Carlo Bicchi[1], Erica Liberto[1], Lucie Baroux[2], Philippe Merle[2], Qingping Tao[3] and Stephen E. Reichenbach[3,4]

[1]Dipartimento di Scienza e Tecnologia del Farmaco, Università degli Studi di Torino, Turin, Italy
[2]Analytical Innovation, Corporate R&D Division, Firmenich S.A. Geneva, Switzerland
[3]GC Image LLC, Lincoln, NE, USA
[4]Computer Science and Engineering Department, University of Nebraska – Lincoln, NE, USA

*Corresponding author:
Dr. Chiara Cordero - Dipartimento di Scienza e Tecnologia del Farmaco, Università di Torino, Via Pietro Giuria 9, I-10125 Torino, Italy – e-mail: chiara.cordero@unito.it; phone: +39 011 6707172; fax: +39 011 2367662

Abstract

The capture of volatiles patterns from food gives access to a high level of information related to the role of several functional variables (origin, processing, shelf-life etc.) on sample composition and quality. This analytical process is a type of *fingerprinting* that captures signals revealing a sample's unique traits in order to make effective comparisons. When the focus is on food volatilome, comprehensive two-dimensional gas chromatography combined with time-of-flight mass spectrometry (GC×GC-TOF MS) is undoubtedly the most effective technique for comprehensive fingerprinting studies. TOF MS combined with Electron Ionization (EI) gives access to characteristic fragmentation patterns that enables high confident analyte identification.

A recently patented ion source, featuring variable-energy EI, when operated at low energies (10 eV, 12 eV, 14 eV), claims enhanced intensity of structure-indicating ions while minimizing the inherent loss of sensitivity traditionally experienced at low EI energies. The acquisition, done by multiplexing between two ionization energies in a single analytical run, generates tandem data streams with complementary natures in terms of both MS pattern signature and relative response.

This study explores the potentials of combined untargeted/targeted (*UT*) fingerprinting based on template matching (i.e., *UT fingerprinting* work-flow) with tandem signals. As a challenging bench-test, the complex volatile fractions of high quality cocoas are analyzed and exploited for discrimination.

The quality of the spectra at 70 eV is confirmed by similarity match factors above the acceptability threshold, fixed at 950, while spectral differences between hard (70 eV) and soft (12 eV, 14 eV) ionization are evaluated in terms of spectral profiles (similarity match factor) and signal-to-noise ratio (SNR). Tandem signals are processed independently and after their fusion in a single stream (summed signal) by the *UT fingerprinting* work-flow. Signal characteristics and 2D-peak indicators (SNR, detectable 2D peaks, spectral peak intensities) are computed and evaluated to define the best strategy.

Classification performance, directed to discriminate raw from roasted cocoa from four different origins, is validated by cross-comparing supervised pattern recognition results (Linear Discriminant Analysis and Partial Least Squares Discriminant Analysis) on the most discriminant 2D-peak features as they are revealed by single ionization channels or from fused data streams. Cross-matching untargeted and targeted data provides additional validation. Classification results indicate the potential for superior performances of *UT fingerprinting* with fused data streams (summed signals), while signal characteristics at low ionization energies not only offer additional elements to better discriminate isomeric analytes but also the chance to achieve wider dynamic range of exploration.

Key-words

52 UT fingerprinting, template matching, tandem ionization, comprehensive two-dimensional gas
53 chromatography, fused data streams
54

1. Introduction

The capture of volatiles patterns from food is a process that, although challenging, gives access to a high level of information related to important variables such as sample composition, origin, processing, shelf-life, and product quality. This process is a type of *fingerprinting* in that it records analytical signals as a sample's distinctive traits, e.g., to make comparisons [1–3]. Therefore, analytical fingerprinting should utilize technologies or platforms that are capable of informing about analytes identities and relative abundances (or quantities) while providing their complete resolution to effectively exploit sample chemical dimensionality [4].

Analytical platforms that combine multidimensional chromatography (MDC) with mass spectrometric detection deliver on these requirements and, if the focus of the research is food volatilome, comprehensive two-dimensional gas chromatography combined with time-of-flight mass spectrometry (GC×GC-TOF MS) is undoubtedly the most effective technique [2,3,5,6]. GC×GC-TOFMS yields highly resolved 2D patterns of volatiles that are distinctive signatures encoding fundamental information about individual samples, particularly analytes identities and relative amounts.

MS with Electron Ionization (EI) produces characteristic fragmentation patterns that, thanks to the availability of general or dedicated commercial databases [7,8], when combined with relative retention data (i.e., linear retention indexes I^T_S), enable reliable identifications of targeted compounds. TOF MS with low mass resolution is the most common detector adopted in combination with GC×GC [5], although qMS with advanced high efficiency sources has gained popularity for its compatibility with routine applications [9,10]. Within the available GC×GC-MS solutions, recent studies, dealing with food sensometabolome or characteristic odorants in natural extracts [11–13], discussed the advantages provided by high-resolution MS (HRMS) that produces exact masses, specific fragments, or mass defects data even when co-elution issues affect chromatographic resolution and therefore quality of the spectral data.

In such systems, soft ionization techniques have the potential to help solving identification ambiguities in those cases where EI produces very similar fragmentation patterns, as for structural isomers. In general, soft ionization preserves information about molecular ions while minimizing associated structural fragmentation [14]. Most of the available soft-ionization techniques, i.e., chemical ionization (CI), field ionization (FI), and photoionization (PI), require dedicated instrumentation and/or ion sources, e.g., to switch from standard EI to CI acquisition. However, recent instrumental solutions perform variable-energy EI feature tandem ionization across single analytical runs.

A recently patented ion source, featuring variable-energy EI, also referred to as Tandem Ionization (TI) [Select eV™ - US patent number 9,786,480], claims enhanced intensity of structure-indicating ions and minimize the inherent loss of sensitivity traditionally experienced at low-energy EI. The ion source applies a high potential difference to accelerate the electrons away from the filament, but then reduces their energy before they arrive in the ion chamber [15]. The acquisition is done by time-switching between two ionization energies in a single analytical run so that two data streams are generated and acquired simultaneously.

Experimental data demonstrated that variable-energy EI was successful to distinguish and identify large isomeric species in unresolved complex mixture (UCM) of motor oil samples [14]. The authors combined data from tandem signals, acquired at 70 eV and 14 eV, together with rationalized 2D retention patterns of aliphatic and aromatic hydrocarbons in the range between C_{12}–$C_{36,}$ to achieve an almost complete chemical characterization of samples.

Dubois et al. [16] explored the composition of light volatile organic compounds (VOCs) mixtures from human blood and tested the beneficial effect of low ionization energies (12, 14 and 16 eV) on analyte fragmentations and on the presence of structurally meaningful ions including molecular ions. The authors confirmed previous evidence of the additional confidence in peak identification, especially for closely eluting isomers, often observed in the profiling of the headspace of blood.

A recent paper by Freye et al. [17] moved a step ahead and provided a proof of concept on tandem ionization at 14 eV and 70 eV, discussing the complementary nature of tandem data streams with respect to data processing opportunities. The authors applied a tile-based Fisher ratio analysis and designed a discovery-based investigation by spiking diesel fuel samples with a mixture of twelve analytes at a nominal concentration of 50 ppm. They were successful in detecting eleven of twelve exogenous analytes by processing the data after fusion of tandem signals.

In this study, we explore, for the first time, the potentials and limitations of pattern recognition approaches based on template matching (i.e., *UT* fingerprinting work-flow [18,19]) applied to tandem signals provided by hard and soft ionization. In particular, this work begins to develop a work-flow that exploits information from hard and soft ionization data streams while keeping the advantages of comprehensively mapping the distributions of known and unknown compounds across samples with great confidence. As a challenging test case, high quality cocoa from different origins and in two stages of processing are considered. The cocoa volatile metabolome, with its high chemical dimensionality [4], poses several challenges for both detailed profiling and comprehensive fingerprinting.

2. Experimental

2.1 Chemicals and cocoa samples

The internal standard (IS) α-thujone for chromatographic areas/volumes normalization was from Sigma Aldrich (Milan, Italy) and dissolved in diethyl phthalate (Sigma Aldrich 99% of purity) at a concentration of 100 mg/L.

The mixture of *n*-alkanes (*n*-C9 to *n*-C25) for calibrating linear retention indices (I^T_S) in the first dimension was from Sigma-Aldrich. The I^T_S solution was prepared in cyclohexane at a concentration of 100 mg/L.

Cocoa samples were provided by Gobino srl (Turin, Italy). Samples were selected on the basis of their specific sensory profile from high-quality productions of different geographic origins. Roasting conditions (time and temperature) were set to achieve optimal flavor. The list of samples, together with their origin, supplier, and harvest year are reported in **Table 1**.

2.2 Headspace Solid Phase Microextraction devices and sampling conditions

The divinylbenzene/carboxen/polydimethylsiloxane 1 cm SPME fiber was from Supelco (Bellefonte, PA, USA) and used for HS-SPME sampling. The standard in-fiber procedure [20] was adopted to preload the IS (α-thujone) onto the fiber before sampling. A 5.0 µL solution of IS (α-thujone at 100 mg L^{-1} in diethyl phthalate) was placed into a 20 mL glass vial and subjected to HS-SPME at 50°C for 5 min. After the IS loading step, the SPME device was exposed to 500 mg of cocoa in a headspace glass vials (20 mL) for 30 min at 50°C. Extracted analytes were recovered by thermal desorption of the fiber into the S/SL injection port of the GC system at 250°C for 5 min.

2.3 GC×GC-TOF MS featuring Tandem Ionization: instrument set-up and conditions

GC×GC analyses were performed on an Agilent 7890B GC unit coupled with a Bench TOF-Select™ system (Markes International, Llantrisant, UK) featuring Tandem EI. For the purposes of this study, hard ionization at 70 eV was set for identity confirmation while lower electron ionization energies were explored in the range 12-16 eV to find optimal conditions for tandem acquisitions. The ion source and transfer line were set at 270°C. The MS optimization option was set to operate in Tandem Ionization with a mass range between 40 and 300 m/z; data acquisition frequency was 50 Hz per channel; filament voltage was set at 1.60 V.

The system was equipped with a two-stage KT 2004 loop thermal modulator (Zoex Corporation, Houston, TX) cooled with liquid nitrogen controlled by Optimode™ V.2 (SRA Instruments, Cernusco sul

Naviglio, MI, Italy). The hot jet pulse time was set at 250 ms, modulation period was 4 s, and cold-jet total flow was progressively reduced with a linear function from 40% of Mass Flow Controller (MFC) at initial conditions to 8% at the end of the run.

2.4 GC×GC columns and settings

The column set was configured as follows: ^{1}D SolGel-Wax column (100% polyethylene glycol; 30 m × 0.25 mm d_c, 0.25 µm d_f) from SGE Analytical Science (Ringwood, Australia) coupled with a ^{2}D OV1701 column (86% polydimethylsiloxane, 7% phenyl, 7% cyanopropyl; 2 m × 0.1 mm d_c, 0.10 µm d_f), from J&W (Agilent, Little Falls, DE, USA). SPME thermal desorption into the GC injector port was under the following conditions: split/splitless injector in split mode at 250°C, split ratio 1:20. The carrier gas was helium at a constant flow of 1.3 mL/min. The oven temperature program was from 40°C (2 min) to 240°C at 3.5°C/min (10 min).

The *n*-alkanes liquid sample solution for I^T_S determination was analyzed under the following conditions: split/splitless injector in split mode, split ratio 1:50, injector temperature 250°C, and injection volume 1 µL.

2.5 Data acquisition and 2D data processing

Data were acquired by TOF-DS software (Markes International, Llantrisant, UK) and processed using GC Image GC×GC Software, ver 2.8 (GC Image, LLC, Lincoln NE, USA).

3. Results and Discussion

In this study, the cocoa volatile metabolome was used as challenging bench test to evaluate potentials and opportunities provided by tandem hard and soft electron ionization in terms of detailed and informative profiling and accurate fingerprinting with template matching algorithms. Based on the outcomes of previous studies aimed at capturing diagnostic fingerprints from high-quality cocoa of different geographical and botanical origin [21–24], it was clear that GC×GC-MS can be employed to deeply explore the multiple chemical dimensions encrypted on the volatile metabolome. Within this fraction are several chemical classes, including informative homologues that are formed through known and unknown chemical and enzymatic pathways during post-harvest and industrial processing. Therefore, the possibility to map and collect informative 2D patterns, i.e., characteristic quali-quantitative distributions of analytes in the multidimensional analytical space, is fundamental. The hyphenation of GC×GC with TOF MS featuring tandem ionization adds a further dimension at the

detection level, providing additional information while opening new opportunities at the data elaboration level [17].

The next subsection describes some preliminary steps designed to evaluate tandem ionization detection reliability and to better understand the complementary nature of tandem signals at 70 eV and lower energies for cocoa application. Spectral quality at 70 eV and spectral similarity/dissimilarity are computed to set optimal parameters for tandem acquisition.

Once tandem ionization acquisition parameters are defined, samples are run in a single analytical batch and 2D data processed by UT fingerprinting [18,19]. A schematic diagram of the UT fingerprinting workflow is illustrated in **Supplementary Figure 1**. Informational features (untargeted and targeted peaks) covering the entire cocoa volatile metabolome, are then computed and some statistical descriptors (2D peaks detection thresholds, signal levels, and Signal-to-Noise Ratio (SNR)) are evaluated. Finally, classification is run on untargeted 2D-peak features from single ionization channels and on fused data streams; then, results are discussed and cross-validated with targeted peak features.

3.1 Tandem ionization: spectral quality at 70 eV and cocoa volatiles information dimensions

As a preliminary step, the reliability of 70 eV spectra acquired featuring tandem ionization at 50 Hz per channel was evaluated. Quality matches were calculated by matching candidate spectra at 70 eV with those collected in commercial databases (NIST 2014 and Wiley 7n) and in in-house databases established from regular single quadrupole measurement, with the positive identification threshold set at 950 of Direct Match Factor (DMF). Linear retention indices I^T_S (± 20 units tolerance) also were considered for identification. In case of co-elutions, spectral deconvolution by the AMDIS algorithm [8] and/or manual inspection with spectral subtraction were performed before identification.

Supplementary Table 1 lists all 193 targeted analytes plus the IS together with their retention times (^1t_R min, ^2t_R sec), experimentally determined I^T_S values, and NIST Identity Search algorithm Match Factors: DMF and Reverse Match Factor (RMF), obtained by considering the Peak Apex average spectrum.

Figure 1 illustrates, as a bar chart of the summed DMF and RMF values (ordered by DMF) for the 192 targeted analytes. On average, DMF achieved 930 similarity and RMF achieved 960. The latter excludes from the computation those m/z fragments that are not present in the reference spectra. Peaks with Peak Apex DMF below 950 were affected by co-elution issues. In those cases, by deconvolution and/or manual spectral subtraction, matches above 950 were obtained (data not shown) confirming that tandem ionization acquisition does not preclude confident identification while adding

214 further information in the soft ionization data stream. Further comments on this aspect are reported in
215 *Section 3.2*.
216
217 **Insert Figure 1 here**
218
219 Within the 193 targeted analytes are several informative chemicals known for their role in the
220 description of cocoa aroma (key-aroma compounds and potent odorants), post-harvest practices, and
221 technological impacts. Within the list of sensory active compounds [25,26] concurring in the definition
222 of cocoa aroma blueprint, twenty were successfully identified: 2-methyl-butanal, ethyl 2-
223 methylbutanoate, 2-heptanol, dimethyl trisulfide, 2,3,5-trimethylpyrazine, acetic acid, 2-ethyl-3,6-
224 dimethyl-pyrazine, 2-ethyl-3,5-dimethyl-pyrazine, 2,3-diethyl-5-methylpyrazine, linalool, 2-methyl
225 propanoic acid, ethyl 2-methylpropanoate, butanoic acid, phenyl acetaldehyde, 3-methyl butanoic acid,
226 1-phenyl ethanol, 2-phenyl ethyl acetate, phenylethyl alcohol, δ-2-decenolactone, and 4-hydroxy-2,5-
227 dimethyl-3(2h)-furanone. Their signature (quali-quantitative distribution) informs about cocoa flavor,
228 imparting characteristic notes as: *earthy, roasted, rancid, sour, sweaty, malty, cocoa, buttery, flowery,*
229 *honey-like, fruity, green, fatty, sulfury,* and *phenolic*.
230 Furthermore, important technological markers [21] and origin tracers [18,26] also were
231 identified: 2,3-butanedione, 2,3-pentanedione, dimethyl disulfide, methyl pyrazine, 3-hydroxy-2-
232 butanone, 1-hydroxy-2-propanone, 2,5-dimethylpyrazine, 2,3-octanedione, 2,6-dimethylpyrazine,
233 ethylpyrazine, 2,3-dimethyl pyrazine, 2-ethyl-6-methylpyrazine, 2-ethyl-5-methylpyrazine, 1-acetyloxy-2-
234 propanone, furfural, tetramethylpyrazine, 2-furan methanol, and (e)-2-phenyl-2-butenal. The residual
235 150 targeted analytes complete the characteristic volatiles signatures, carrying information about
236 additional variables (covering most of the key steps impacting on cocoa chemical composition along the
237 production chain) although their specific roles are not yet validated.
238 Such a comprehensive chemical characterization of the sample volatilome is greatly attractive,
239 especially for those studies of interactions of multiple variables. Therefore, some key-performance
240 parameters have to be evaluated for their impact on fingerprinting effectiveness: specificity, sensitivity,
241 and dynamic range of the response are fundamental since tandem ionization could provide additional
242 advantages if properly set.
243 Since spectral quality at 70 eV was confirmed as satisfactory, providing proofs on adequate
244 method reliability at the detection level, the successive step was the selection of tandem acquisition
245 ionization energies capable of providing complementary information at spectral level [14,17,27]In this

perspective, spectral similarity/dissimilarity between different ionization energies was considered to define the best conditions. The next section focuses, for a selection of informative chemicals, on spectral differences at 12 and 14 eV and discusses dissimilarity between hard and soft ionization spectra, including some considerations about SNR values and consequent method sensitivity and dynamic range.

3.2 Tandem ionization: spectral dissimilarity and complementary nature of tandem signals

The effect of different ionization voltages on spectral profiles was evaluated by recording spectra at 12 and 14 eV. Lower energies (10 eV) were excluded because of a dramatic drop in signal intensities. **Table 2** lists DMF and RMF values for a series of targeted analytes representative of different chemical classes or series of homologues, for spectral comparisons between: a) 70 eV *vs.* database (Wiley 7n or NIST 2014); b) 12 eV *vs.* 14 eV; c) 12 eV *vs.* 70 eV; d) 14 eV *vs.* 70 eV.

Results indicate, as expected, that on average, the spectral dissimilarity between 12 eV and 70 eV is higher compared to that between 14 and 70 eV. The average DMF was 779 at 12 eV and 830 at 14 eV. Interestingly, several analytes spectra at 12 and 14 eV are characterized by the same fragments although with different relative abundance; this is true for those analytes that reported identical values for DMF and RMF: 2,3-pentanedione, 3-penten-2-one, limonene, benzaldehyde, 2-furan methanol, and benzyl alcohol. The same situation is evident also between spectra at 12 and 14 eV *vs.* 70 eV for 2,3-pentanedione, 3-penten-2-one, benzaldehyde, 2-furan methanol, benzyl alcohol, γ-octalactone, 1h-pyrrole-2-carboxaldehyde, and γ-nonalactone.

Within the analytes that showed the most dissimilar patterns (lower DMF values), nonanal and limonene are illustrated in **Figure 2**. For nonanal (**Fig. 2A**), lower ionization energies revealed the molecular ion (i.e, 142 m/z) that was not present at 70 eV. Additionally, on the spectrum at 12 eV, the base peak was 98 m/z while at 14 eV and 70 eV, the most abundant fragment was 57 m/z. For limonene (**Fig. 2B**), a terpenoid derivative, lower ionization energies produced higher relative abundances for fragments with higher m/z ratios (i.e., 93, 107 and 121 m/z) and the molecular ion (i.e., 136 m/z) is enhanced.

Insert Figure 2 here

Lower ionization energies produce fewer fragments, therefore resulting in lower spectral/signal intensities. However, for those analytes that showed reduced fragmentation at lower eV, the resulting signals are enhanced and consequently SNR may be improved compared to higher energies.

Table 2 reports the SNR values for a selection of targets registered from tandem signals at 70 and 12 eV from a roasted Ecuador cocoa. Streker aldehydes (2-, and 3- methylbutanal), furan derivatives (furfural and 2-furan methanol), and benzaldehyde have higher relative intensities at 12 eV. This interesting pattern, also seen for other analytes (data not shown), evidences the complementary nature of tandem ionization signals and, in this case as quantitative indicator, suggests that lower ionization energies may be beneficial for fingerprinting sensitivity extending the dynamic range of detection. For analytes where 70 eV produces higher SNRs, detector saturation may therefore be a limiting factor and, in these cases, the tandem signal at lower eV may compensate for this.

In this perspective, where the complementary nature of tandem signals has been established by comparing several analytes features, it is of interest to test the effectiveness of comprehensive chromatographic fingerprinting conducted on tandem signals independently or after their fusion in single data streams. The next section evaluates informational features over the entire volatile metabolome (untargeted and targeted peaks) through some statistical descriptors: 2D peaks detection thresholds, signal levels, and SNR.

3.3 Tandem signals informational features

Cocoa samples from four different origins and two processing stages (raw and roasted) analyzed in duplicate are considered here for the processing. Each of the 16 runs (4×2×2) produced a chromatogram for each ionization level (12eV and 70eV), resulting in 32 directly acquired chromatograms. To assess the possibility of increasing performance by combining the data for the two ionization levels (i.e., data fusion), an additional 16 chromatograms were created by adding the two directly acquired chromatograms for each run. So, in total, 48 chromatograms from 16 runs on eight samples were analyzed.

3.3.1 2D-peak detection

An important step in the *UT fingerprinting* workflow [18,19] is to establish a set of reliable peaks that can be used for alignment, in order to obtain consistent features across a set chromatograms, even in the presence of retention-times variations. In this step, a relatively high SNR peak-detection threshold of 100 was applied as the acceptable limit to the ratio of the total intensity count (TIC) of the apex spectrum to the standard deviation of background noise TIC. Then, composite chromatograms were computed as the sums of the sets of aligned chromatograms for 12 eV, 70 eV, and summed data. These three composite chromatograms are shown in **Figure 3**. Note that adding the chromatograms to create

a composite not only yields a single chromatogram to which all compounds in all samples contribute, but also attenuates random-noise variations, thereby increasing SNR.

Insert Figure 3 here

With the threshold SNR ≥ 100, 335 2D-peaks (blobs) were detected in the composite of 12 eV chromatograms, 491 blobs were detected in the composite of 70 eV chromatograms, and 498 blobs were detected in the composite of summed chromatograms. These results, shown in the top row of **Table 3**, indicate that more high-SNR 2D-peaks are produced by 70 eV ionization than by 12 eV ionization. The number of detected high-SNR 2D-peaks was largest in the composite of summed chromatograms.

When analyzing individual chromatograms (e.g., to be matched with a UT template), a relatively low SNR peak-detection threshold may be appropriate so as not to miss compound peaks even at the cost of false detections. The lower part of **Table 3** shows the number of 2D-peaks (or blobs) detected in each of the individual chromatograms with the SNR ≥ 20, as well as the averages by ionization energy and sample source region. With the low SNR threshold, about 70% more 2D-peaks were detected, on average, in the 12 eV chromatograms than in the 70 eV chromatograms, with an average of 777 2D-peaks detected with 12 eV and 451 2D-peaks detected with 70 eV. However, as shown by the example chromatograms in **Figure 4**, many of the additional 2D-peaks are in noisy regions and appear to be false detections (**Fig. 4A**). In the summed chromatograms (**Fig. 4C**), more 2D-peaks are detected than with 70 eV, but fewer than with 12 eV. As detailed below, the average signal intensities in the 12 eV chromatograms are lower than in the 70 eV chromatograms.

Insert Figure 4 here

With respect to the cocoa volatiles patterns, on average, a few more 2D-peaks were detected from the roasted samples than the raw samples. However, although more 2D-peaks were detected in the roasted samples from Colombia and Ecuador, more 2D-peaks were detected in the raw samples from Mexico and Sao Tome. The Sao Tome samples yielded the most 2D-peaks, indicating a higher chemical complexity, followed by samples from Mexico, Colombia, and Ecuador, with about 16% more 2D-peaks in the Sao Tome samples than those from Ecuador. Differences of volatiles signatures are in line with previous studies [21] where it was confirmed the pre-eminent role of botanical/geographical origin over

processing in the chemical dimensionality of samples. Roasting on cocoa triggers several chemical reactions that result in more "quantitative" changes on volatiles signatures rather than "qualitative" differences.

3.3.2 Signal intensity

Signal levels were analyzed in each of the peak-regions derived from the composite of summed chromatograms (shown in **Figure 3C**). Signal levels were substantially greater in the 70 eV chromatograms than in the 12 eV chromatograms. In the individual chromatograms, on average, the peak-region TIC apexes in the 12 eV chromatograms were only about 30% of the same peak-region TIC apexes in the 70 eV chromatograms. The peak-region TIC apex in the summed chromatograms averaged 126% of the peak-region apex TIC with 70 eV. On average, the peak-region TIC volumes in the 12 eV chromatograms were only 40% of the same peak-region volumes in the 70 eV chromatograms. The peak-region TIC volumes in the summed chromatograms averaged 124% of the peak-region volume with 70 eV. It appears that the ratios of the 12 eV to 70 eV peak-region volumes (40%) are larger than the ratios of the 12 eV to 70 eV apexes (30%) because lower intensity spectra are relatively less different between the two ionization energies (so, the off-apex spectra are less different than are the apex spectra). Spectral differences are discussed below.

3.3.3 Spectral peak intensities

From each peak-region in the composite of summed chromatograms, two spectral channels were selected to evaluate spectral intensities: (1) the channel of the base peak (i.e., the *m*/*z* of the largest intensity component in apex spectrum), and (2) a large-mass candidate for the molecular ion (selected as the largest *m*/*z* with relative intensity of at least 10% of the base peak intensity, with the additional constraint to filter isotopes that the unit mass interval just below did not have a larger intensity peak).

Just as for the TIC intensities, the base peak intensities were substantially greater in the 70 eV chromatograms than in the 12 eV chromatograms. On average, peak-region apex base-peak intensities in the 12 eV chromatograms were only 29% of the peak-region apex base-peak intensities in the 70 eV chromatograms. The peak-region apex base-peak intensities in summed chromatograms averaged 128% of the peak-region apex base-peak intensities with 70 eV. On average, peak-region base-peak volumes in the 12 eV chromatograms were only 17% of the peak-region base-peak volumes in the 70 eV chromatograms. The peak-region base-peak volume in the summed chromatograms averaged 116% of the peak-region base-peak volume with 70 eV.

Similarly, the large-mass-peak intensities were substantially greater in the 70 eV chromatograms than in the 12eV chromatograms, but the difference was smaller than for the base-peak intensities. On average, peak-region apex large-mass-peak intensities in the 12 eV chromatograms were 60% of the peak-region apex large-mass-peak intensity in the 70 eV chromatograms. The peak-region apex large-mass-peak intensities in summed chromatograms averaged 158% of the peak-region apex large-mass-peak intensities with 70eV. On average, peak-region large-mass-peak volumes in the 12 eV chromatograms were only 43% of the peak-region large-mass-peak volumes in the 70 eV chromatograms. The peak-region large-mass-peak volume in the summed chromatograms averaged 142% of the peak-region large-mass-peak volume with 70 eV.

This is an interesting result if we consider the higher informative power of large-mass-peaks in a spectrum. This characteristic relates to the specificity of lower ionization energies and so provides foundation for the adoption of low eV data stream for effective fingerprinting as well as for the added value it brings when summed to the 70 eV channel.

3.3.4 Signal-to-noise: SNR and VNR

On average, the TIC background noise for 12 eV was approximately 33% of the noise for 70 eV and the noise in the summed chromatograms was about 105% of the noise for 70eV. With the lower signal and noise levels for 12 eV, the average peak SNR (TIC apex intensity to noise standard deviation) for 12 eV was about 86% of the SNR with70 eV. However, the average volume-to-noise ratio (VNR) with 12 eV was about 134% of the VNR with 70 eV. The SNR of the summed chromatograms was about 115% of the SNR with 70eV and the VNR of the summed chromatograms about 117% of the VNR with 70 eV.

The spectral background noise was fairly consistent at most m/z levels, but, at some m/z levels, especially smaller m/z levels, the raw spectral background noise was substantially larger with 70 eV than with 12 eV, as illustrated in **Supplementary Figure 2**. However, baseline correction can detect and attenuate large baseline spectral values, as illustrated in **Supplementary Figure 3**.

3.4 Classification performance

3.4.1 Fisher Discriminant Ratios of Individual Features in Individual Peak-Regions

The potential of individual features for classification is indicated by the Fisher Discriminant Ratio (FDR), the ratio of the scatter between classes to the scatter within classes. Classification was part of the automated work-flow applied on single and summed data streams within the Image Investigator™ (GC Image). For the 498 peak-regions extracted from untargeted analysis of the composite of summed

406 chromatograms, various features could be used for discrimination. Seven computed peak-region
407 features were analyzed: volume (summed response for all modulated peaks included in a defined peak-
408 region), percent response (volume to total chromatogram response), apex response (highest modulation
409 response), base-peak apex response (response related to most intense m/z fragment from highest
410 modulation), base-peak volume (peak-region volume related to most intense m/z fragment), large-mass
411 apex response (response related to largest m/z fragment from highest modulation), and large-mass
412 volume (peak-region volume related to most intense m/z fragment).

413 For all of these features, most peak-regions have relatively small FDR, i.e., are weak indicators of
414 class differences. As shown in **Table 4**, the average FDR for different features ranged from 0.31 for apex
415 response with 12 eV to 0.54 for percent response with 12 eV. The median FDR was far below the mean,
416 ranging from 0.02 for volume with 12 eV to 0.32 for percent response with 12 eV. For five of the seven
417 computed features, the average FDR with 70 eV was larger than with 12 eV, whereas only one feature
418 had a larger average FDR with 12 eV (and the average FDRs were nearly identical for each feature). The
419 average FDR for the summed chromatograms was about the same as with 70 eV.

420 Although there can be useful information in many weakly indicative features, most of the potential
421 for classification exists within a relatively small number of features. The maximum FDR ranged from 2.92
422 for the large-mass peak intensity with 12 eV to 14.01 for the percent response with 70 eV. For six of the
423 seven features, the maximum FDR with 70 eV was larger than with 12 eV and about the same as with
424 the summed chromatograms. The average of the top-ten FDRs for each feature ranged from 3.01 for the
425 large-mass peak intensity with 12 eV to 5.51 for the percent response with 70 eV. For six of the seven
426 features, the top-ten FDR average was greater with 70 eV than with 12 eV. The top-ten FDR average for
427 the summed chromatograms was larger than with 70 eV for four of the seven features.

428 As the basis for classification, percent response is clearly the most promising of the seven features,
429 producing the largest FDR (14.01 with 70 eV), the largest top-ten FDR average (5.51 with 70 eV), and
430 largest mean FDR (0.54 with 12 eV). However, base-peak volume was the best performing feature with
431 12 eV for maximum FDR and top-ten FDR average (7.80 and 4.96, respectively).

432 Percent response also has some intrinsic advantages being a peak feature that refers to normalized
433 data therefore enabling consistent comparative analysis even without external standard/internal
434 standard normalization of analytes responses. On the other side, base-peak volume is more sensitive to
435 “true” quantitative response variations across chromatograms and has the advantage of informing
436 about single analyte fluctuations in more detail.

437

3.4.2 Linear Discriminant Analysis on untargeted features from tandem signals

As anticipated by the FDR analysis, percent response provided the best basis for classification by linear discriminant analysis (LDA), and was the only feature to support 100% classification accuracy in leave-one-out trials with the chromatograms from raw and roasted samples. The next best classification accuracy was 93.75% for both base-peak and large-mass volume with 12eV. The LDA scores with inferential Gaussian distributions for the leave-one-out trials are shown in **Supplementary Figure 4**. In the cross-validation experiments, replicates were left out together to prevent bias. The Fisher ratio for the LDA scores were 2.99 for the summed chromatograms, 2.75 with 70 eV, and 2.71 with 12 eV, which is not a very large range, but does indicate that better discrimination can be achieved with the fused/summed data.

Concerning cocoa analysis, the roasted samples had much more variable LDA scores than did the raw samples (as seen in **Supplementary Figure 4**). Within the roasted samples, the LDA scores of samples from Mexico were the most different from the raw samples scores (leftmost in **Supplementary Figure 4**) and the LDA scores of the samples from Ecuador were the closest to the raw samples scores. Many of the same peak-regions were significant (large score-weighted standard deviations) with 12 eV, 70 eV, and the summed chromatograms, with six features in the top-10 for all three classification schemes and four other features in the top-10 for two of the three classification schemes. The top-ten peak-regions for LDA classification with summed chromatograms are listed in **Table 5.** Of the other four peak-regions that appeared in the top-ten of only one scheme, all were in the top-40 for the other two schemes. However, two of the top-10 features with both 70 eV and summed chromatograms were not highly significant with the 12 eV data: peak-regions #68 and #102 ranked 138 and 177 among 12 eV features.

3.5 Untargeted-Targeted UT fingerprinting: results validation

Results obtained by untargeted fingerprinting on tandem signals elaborated separately or after their summation in a derived data stream were validated against the targeted approach. This step enables objective evidence on discrimination performances of tandem data after fusion taking as benchmark results obtained through the well-established work-flow based on template matching of targeted analytes guided by analyst supervision [28,29]. Supervision was here necessary for those analytes that were affected by co-elution issues (section 3.1); therein, deconvolution and/or manual spectral subtraction were performed to achieve confident identification while informative fragments were selected to isolate analytes response from low-resolved peak-regions. The data matrix for the targeted analytes was obtained by collecting percent responses (the 2D-peak/2D peak-region feature connoted

by a higher information potential – section 3.3.1) for the 193 reliable analytes at 70 and 12 eV ionization energies.

Partial Least Squares – Discriminant Analysis (PLS-DA) was adopted at this stage and, to define informative variables, Variable Importance on the Projections (VIPs) was used to rank targeted analytes on the basis of their power to discriminate between raw and roasted cocoa samples. **Figure 5** shows the first 20 target analytes ranked for their relevance in the discrimination and deriving from the elaboration of 70 and 12 eV data streams independently. In parentheses are the LDA ranking obtained from the untargeted processing of the summed signals (from **Table 5**).

Insert Figure 5 here

Notably, the targeted approach validates the information power of those analytes that were selected by LDA on untargeted features distribution on summed signals (**Table 5**): the top-10 most relevant variables were included in the list of the first top-20 targets with the highest informative power. In addition, within the top-20 analytes highly ranked after PLS-DA on targetes, 3-hydroxy-2-butanone, 2,3-pentanedione, 1-hydroxy-2-propanone, 2,3-dimethyl pyrazine, tetramethylpyrazine, and 2-furan methanol have their informative power cross-validated between tandem data streams. At 12 eV, within the top-20 additional analytes, additional targets are evidenced: 5-methyl-2(5H)-furanone, dodecanal, ethyl 2-methylbutanoate, and 2,6-dimethylpyrazine while at 70 eV those with high relevance are 2-hydroxy-3-pentanone, methyl 2-hydroxypropanoate, dimethyl disulfide, and 2-methyl pyrazine.

The cross-validation of fingerprinting results confirms, once again, the complementary nature of tandem signals: whichever is the data stream (12 or 70 eV) treated as such or as sum of signals, or the approach (untargeted/unsupervised or targeted/supervised) there is univocal identification of discriminant features (untargeted peaks or known analytes) even in such a complex context where confounding variables play a great role (origin and post-harvest practices above all). The advantages of supervised elaborations, as in the case of targeted analysis, are evident for those analytes where co-elution occur; in these cases, single analyte response has to be isolated from co-eluents to achieve adequate specificity. The differential response between tandem signals extends dynamic range of the detector resulting in a larger group of candidates, when tandem signals are combined, to be screened for their information power.

4. Conclusions

The present study gives foundations for a full exploitation of the complementary nature of tandem signals obtained by adopting variable EI energies for UT fingerprinting. The cross-comparison of several 2D peak features and signal characteristics demonstrates that signal fusion (i.e., summed signals) enables effective untargeted fingerprinting leading also to a good discrimination potential of the methodology even in very complex samples. The targeted fingerprinting, driven by analyte supervision during data pre-processing, better exploits the complementary nature of tandem signals due to their differential informative content. In addition, multiplexing tandem ionization during a single analytical run, does not impact on confident analytes identification while offering additional elements to better discriminate isomeric analytes. The improved SNR registered for some analytes at lower ionization energies, is an interesting performance characteristic of the method that can achieve a wider dynamic range of exploration.

Funding

The research was carried out thanks to the financial support of Firmenich S.A. Geneva, Switzerland.

Compliance with ethical standards Notes

Prof. Stephen E. Reichenbach and Dr. Qingping Tao have a financial interest in GC Image, LLC.

Lucie Baroux and Philippe Merle are employees of Firmenich S.A. Geneva, Switzerland.

References

[1] S.E. Reichenbach, X. Tian, C. Cordero, Q. Tao, Features for non-targeted cross-sample analysis with comprehensive two-dimensional chromatography, J. Chromatogr. A. 1226 (2012) 140–148. doi:10.1016/j.chroma.2011.07.046.

[2] C. Cordero, J. Kiefl, P. Schieberle, S.E. Reichenbach, C. Bicchi, Comprehensive two-dimensional gas chromatography and food sensory properties: Potential and challenges, Anal. Bioanal. Chem. 407 (2015) 169–191. doi:10.1007/s00216-014-8248-z.

[3] C. Cordero, J. Kiefl, S.E. Reichenbach;, C. Bicchi, Characterization of odorant patterns by comprehensive two-dimensional gas chromatography: a challenge in omic studies, Trends Anal. Chem. (2018).

[4] J.C. Giddings, Sample dimensionality: A predictor of order-disorder in component peak distribution in multidimensional separation, J. Chromatogr. A. 703 (1995) 3–15. doi:10.1016/0021-9673(95)00249-M.

[5] P.Q. Tranchida, I. Aloisi, B. Giocastro, L. Mondello, Current state of comprehensive two-dimensional gas chromatography-mass spectrometry with focus on processes of ionization, TrAC - Trends Anal. Chem. 105 (2018) 360–366. doi:10.1016/j.trac.2018.05.016.

[6] C. Cordero, H.G. Schmarr, S.E. Reichenbach, C. Bicchi, Current Developments in Analyzing Food Volatiles by Multidimensional Gas Chromatographic Techniques, J. Agric. Food Chem. 66 (2018) 2226–2236. doi:10.1021/acs.jafc.6b04997.

[7] R.P. Adams, Identification of Essential Oil Components by Gas Chromatography—Mass Spectroscopy, Allured Publishing, New York, 1995.

[8] NIST/EPA/NIH Mass Spectral Library with Search Program Data Version: NIST v17, (n.d.).

[9] E. Belhassen, D. Bressanello, P. Merle, E. Raynaud, C. Bicchi, A. Chaintreau, C. Cordero, Routine quantification of 54 allergens in fragrances using comprehensive two-dimensional gas chromatography-quadrupole mass spectrometry with dual parallel secondary columns. Part I: Method development, Flavour Fragr. J. 33 (2018) 63–74. doi:10.1002/ffj.3416.

[10] C. Cordero, P. Rubiolo, S.E. Reichenbach, A. Carretta, L. Cobelli, M. Giardina, C. Bicchi, Method translation and full metadata transfer from thermal to differential flow modulated comprehensive two dimensional gas chromatography: Profiling of suspected fragrance allergens, J. Chromatogr. A. 1480 (2017) 70–82. doi:10.1016/j.chroma.2016.12.011.

[11] Y. Duan, F. Zheng, H. Chen, M. Huang, J. Xie, F. Chen, B. Sun, Analysis of volatiles in Dezhou Braised Chicken by comprehensive two-dimensional gas chromatography/high resolution-time of

554 flight mass spectrometry, LWT - Food Sci. Technol. 60 (2015) 1235–1242.
555 doi:10.1016/j.lwt.2014.09.006.
556 [12] Y.F. Wong, P. Perlmutter, P.J. Marriott, Untargeted metabolic profiling of Eucalyptus spp. leaf oils
557 using comprehensive two-dimensional gas chromatography with high resolution mass
558 spectrometry: Expanding the metabolic coverage, Metabolomics. 13 (2017) 1–17.
559 doi:10.1007/s11306-017-1173-3.
560 [13] D.D. Yan, Y.F. Wong, L. Tedone, R.A. Shellie, P.J. Marriott, S.P. Whittock, A. Koutoulis,
561 Chemotyping of new hop (Humulus lupulus L.) genotypes using comprehensive two-dimensional
562 gas chromatography with quadrupole accurate mass time-of-flight mass spectrometry, J.
563 Chromatogr. A. (2017). doi:10.1016/j.chroma.2017.08.020.
564 [14] M.S. Alam, C. Stark, R.M. Harrison, Using Variable Ionization Energy Time-of-Flight Mass
565 Spectrometry with Comprehensive GC??GC to Identify Isomeric Species, Anal. Chem. 88 (2016)
566 4211–4220. doi:10.1021/acs.analchem.5b03122.
567 [15] Markes International, Select-eV: The next generation of ion source technology, Tech. Note.
568 Applicatio (2016).
569 [16] L.M. Dubois, K.A. Perrault, P.H. Stefanuto, S. Koschinski, M. Edwards, L. McGregor, J.F. Focant,
570 Thermal desorption comprehensive two-dimensional gas chromatography coupled to variable-
571 energy electron ionization time-of-flight mass spectrometry for monitoring subtle changes in
572 volatile organic compound profiles of human blood, J. Chromatogr. A. 1501 (2017) 117–127.
573 doi:10.1016/j.chroma.2017.04.026.
574 [17] C.E. Freye, N.R. Moore, R.E. Synovec, Enhancing the chemical selectivity in discovery-based
575 analysis with tandem ionization time-of-flight mass spectrometry detection for comprehensive
576 two-dimensional gas chromatography, J. Chromatogr. A. 1537 (2018) 99–108.
577 doi:10.1016/j.chroma.2018.01.008.
578 [18] F. Magagna, L. Valverde-Som, C. Ruíz-Samblás, L. Cuadros-Rodríguez, S.E. Reichenbach, C. Bicchi,
579 C. Cordero, Combined untargeted and targeted fingerprinting with comprehensive two-
580 dimensional chromatography for volatiles and ripening indicators in olive oil, Anal. Chim. Acta.
581 936 (2016) 245–258. doi:10.1016/j.aca.2016.07.005.
582 [19] D. Bressanello, E. Liberto, M. Collino, F. Chiazza, R. Mastrocola, S.E. Reichenbach, C. Bicchi, C.
583 Cordero, Combined untargeted and targeted fingerprinting by comprehensive two-dimensional
584 gas chromatography: revealing fructose-induced changes in mice urinary metabolic signatures,
585 Anal. Bioanal. Chem. (2018). doi:10.1007/s00216-018-0950-9.

586 [20] Y. Wang, J. O'Reilly, Y. Chen, J. Pawliszyn, Equilibrium in-fibre standardisation technique for solid-
587 phase microextraction, J. Chromatogr. A. 1072 (2005) 13–17. doi:10.1016/j.chroma.2004.12.084.
588 [21] F. Magagna, A. Guglielmetti, E. Liberto, S.E. Reichenbach, E. Allegrucci, G. Gobino, C. Bicchi, C.
589 Cordero, Comprehensive Chemical Fingerprinting of High-Quality Cocoa at Early Stages of
590 Processing: Effectiveness of Combined Untargeted and Targeted Approaches for Classification
591 and Discrimination, J. Agric. Food Chem. 65 (2017) 6329–6341. doi:10.1021/acs.jafc.7b02167.
592 [22] F. Magagna, E. Liberto, S.E. Reichenbach, Q. Tao, A. Carretta, L. Cobelli, M. Giardina, C. Bicchi, C.
593 Cordero, Advanced fingerprinting of high-quality cocoa: Challenges in transferring methods from
594 thermal to differential-flow modulated comprehensive two dimensional gas chromatography, J.
595 Chromatogr. A. (2018). doi:10.1016/j.chroma.2017.07.014.
596 [23] E.M. Humston, Y. Zhang, G.F. Brabeck, A. McShea, R.E. Synovec, Development of a GCxGC-TOFMS
597 method using SPME to determine volatile compounds in cacao beans, J. Sep. Sci. 32 (2009) 2289–
598 2295. doi:10.1002/jssc.200900143.
599 [24] L.F. Oliveira, S.C.G.N. Braga, F. Augusto, J.C. Hashimoto, P. Efraim, R.J. Poppi, Differentiation of
600 cocoa nibs from distinct origins using comprehensive two-dimensional gas chromatography and
601 multivariate analysis, Food Res. Int. 90 (2016) 133–138. doi:10.1016/j.foodres.2016.10.047.
602 [25] F. Frauendorfer, P. Schieberle, P.E.S. Chieberle, Changes in Key Aroma Compounds of Criollo
603 Cocoa Beans During Roasting Changes in Key Aroma Compounds of Criollo Cocoa Beans During
604 Roasting, J. Agric. Food Chem. 56 (2008) 10244–10251. doi:10.1021/jf802098f.
605 [26] E.O. Afoakwa, A. Paterson, M. Fowler, A. Ryan, Flavor formation and character in cocoa and
606 chocolate: A critical review, Crit. Rev. Food Sci. Nutr. 48 (2008) 840–857.
607 doi:10.1080/10408390701719272.
608 [27] E. Commission, Commission Decision 2002/657/EC implementing Council Directive 96/23/EC
609 concerning the performance of analytical methods and the interpretation of results, Off. J. Eur.
610 Union. L221 (2002) 8–36. http://www.ecolex.org/ecolex/ledge/view/RecordDetails?id=LEX-
611 FAOC049615&index=documents%5Cnfile://g/R&D/PAPE/articles/Mass Spec/European directive
612 MS IP.pdf.
613 [28] J. Kiefl, C. Cordero, L. Nicolotti, P. Schieberle, S.E. Reichenbach, C. Bicchi, Performance evaluation
614 of non-targeted peak-based cross-sample analysis for comprehensive two-dimensional gas
615 chromatography-mass spectrometry data and application to processed hazelnut profiling, J.
616 Chromatogr. A. 1243 (2012) 81–90. doi:10.1016/j.chroma.2012.04.048.
617 [29] C. Cordero, C. Bicchi, P. Rubiolo, Group-type and fingerprint analysis of roasted food matrices

(coffee and hazelnut samples) by comprehensive two-dimensional gas chromatography, J. Agric. Food Chem. 56 (2008) 7655–7666. doi:10.1021/jf801001z.

Figure Captions

Figure 1: bar chart showing the sum of NIST Identity Search algorithm Match Factors: Direct Match Factor (DMF – blue bars) and Reverse Match Factor (RMF – orange bars) for the 192 targeted analytes. Ordering follows descending order of DMF values.

Figure 2: Spectral profiles for nonanal (**2A**) and limonene (**2B**) at 70 eV, 12 eV and 14 eV. Spectral comparisons are between 12 eV and 14 eV (**2A-I** and **2B-I**; between 12 eV and 70 eV (**2A-II** and **2B-II**) and between 14 eV and 70 eV (**2A-III** and **2B-III**). Green text below spectra refers DMF and RMF values.

Figure 3: composite 2D chromatograms obtained by summing single ionization energies channels (12 eV and 70 eV) runs (**3A** and **3B**) or both channels (12 eV + 70 eV) after alignment. 2D-peaks connoted by a cyan rounded shapes are those positively matched in all-but-one chromatogram of the set, e.g., reliable peaks while red rounded shapes indicate 2D-peaks detected in just few chromatograms.

Figure 4: single channel chromatograms from Ecuador samples acquired at 12 eV (**4A**) at 70 eV (**4B**) or after single data stream fusion (**4C**). Effect of SNR variable threshold on 2D-peaks detection. See text for details.

Figure 5: histograms reporting the first twenty most informative analytes (Variable Importance for Projections VIPs) revealed by PLS-DA on targeted peaks (roasted *vs.* raw cocoa). Analytes are reported together with their ranking (in parentheses Sum#n) as resulted by classification analysis of untargeted features on fused data streams. Blue bars refer to 70 eV data while red bars are from 12 eV data,

Table Captions:

Table 1: Cocoa samples under study, together with their origin, supplier, and harvest year.

Table 2: Direct and Reverse Match Factor (DMF and RMF) values for a series of targeted analytes representing different functionalities. Data refers of spectral similarity between 70 eV *vs.* database (Wiley 7n or NIST 2014); b) 12 eV *vs.* 14 eV; c) 12 eV *vs.* 70 eV; d) 14 eV *vs.* 70 eV. Signal-to-noise ratio (SNR) values are those corresponding to peak-apex and recorded at 12 and 70 eV. Their ratio (12 eV / 70 eV) is also reported to facilitate comparisons.

Table 3: number of detected 2D-peaks (blobs) above a certain SNR threshold from composite chromatograms (SNR ≥ 100 for 70 eV, 12 eV, and summed signals) and from single analytical runs (SNR≥ 20 for 70 eV, 12 eV, and summed signals.

Table 4: average Fisher Discriminant Ratio (FDR) values for different peak-region features at 12 and 70 eV and on summed signals. Q1 is the spectral base-peak quantifier ion and Q2 is the large-mass-peak quantifier ion.

Table 5: list of the ten most discriminant 2D-peak regions as indicated by LDA analysis of the summed chromatograms. Data is reported together with unique 2D-peak regions identification numbering (#n), compound name, retention times, and ordinal significance rank within the classification scenarios (Summed, 70 eV, and 12 eV).

Figure 1 color and BW

Figure 1

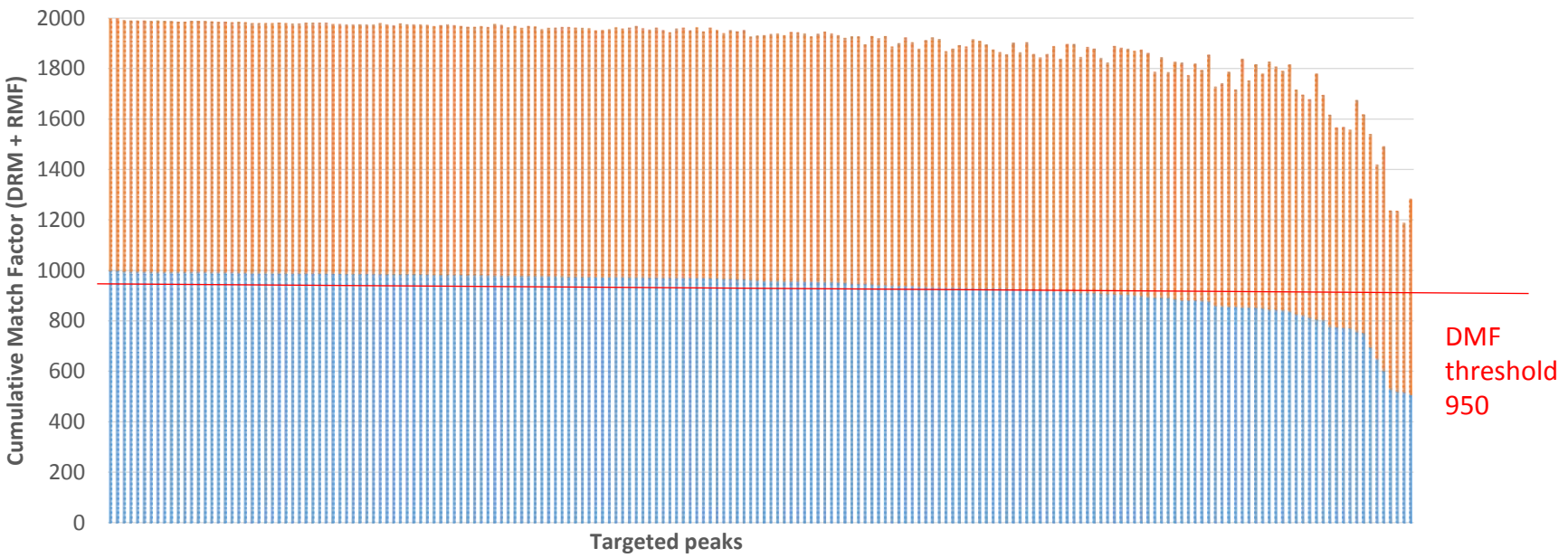

Figure 1

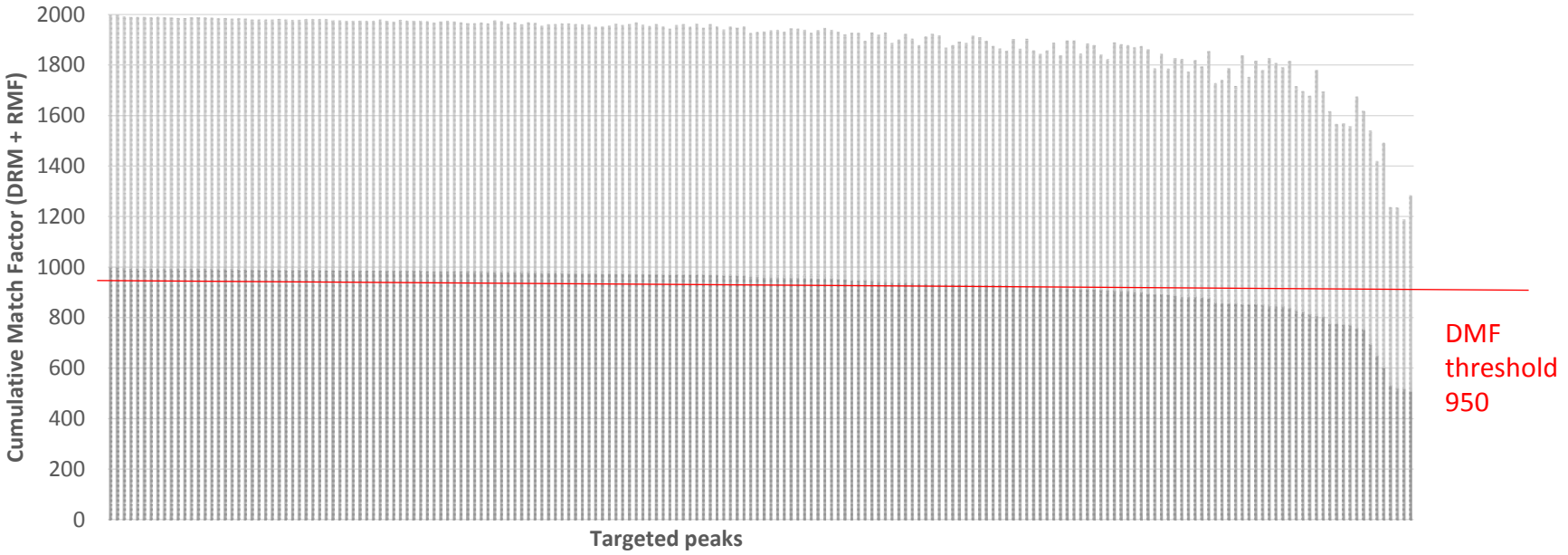
2000
1800
1600
1400
1200
1000
800
600
400
200
0
Cumulative Match Factor (DRM + RMF)
Targeted peaks
DMF
threshold
950

Figure 2 color and BW

Figure 2

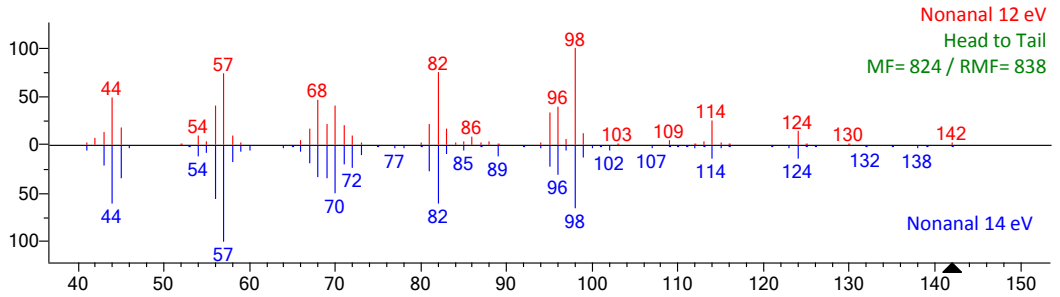

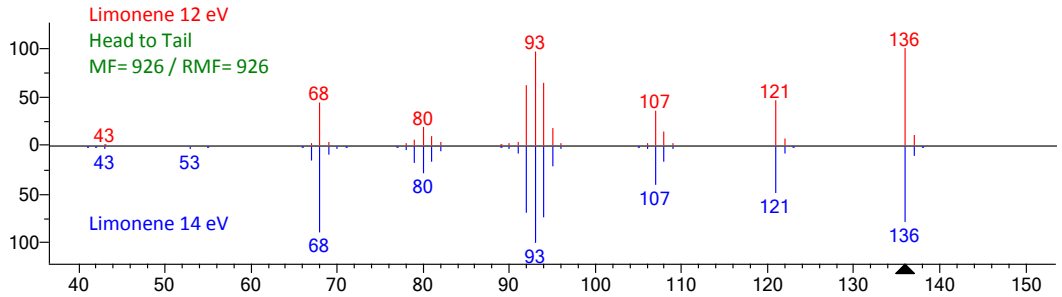

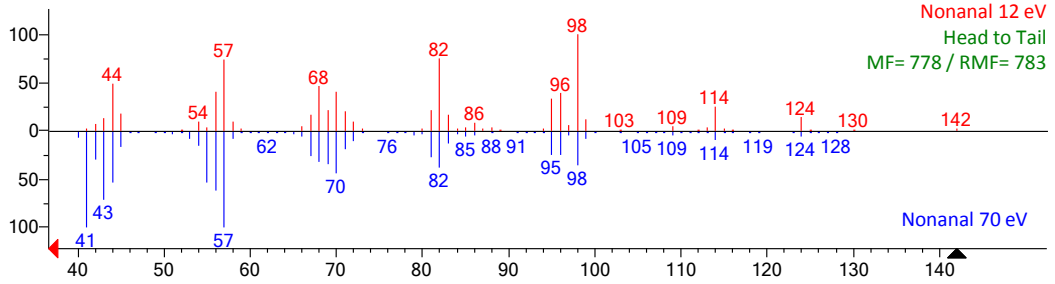

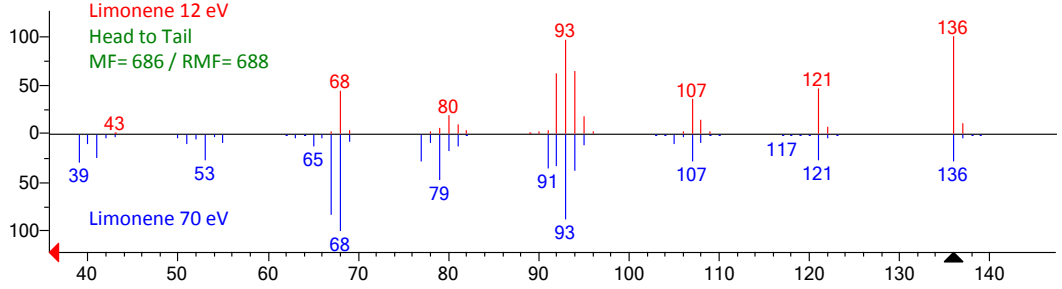

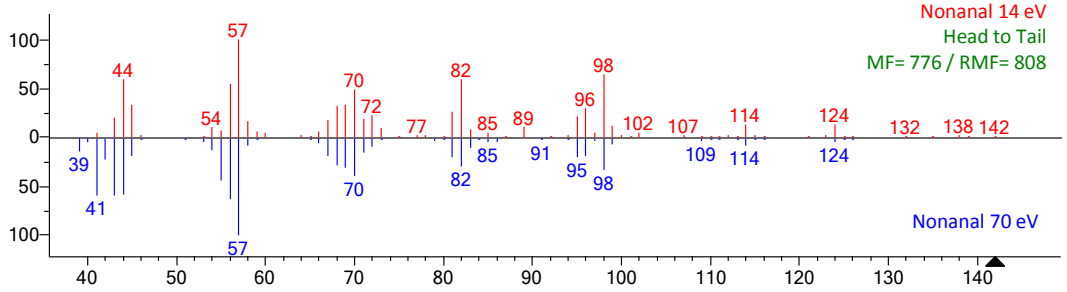

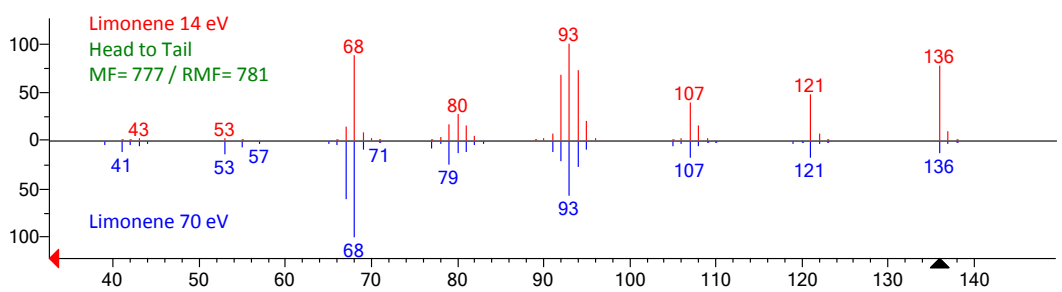

Figure 2

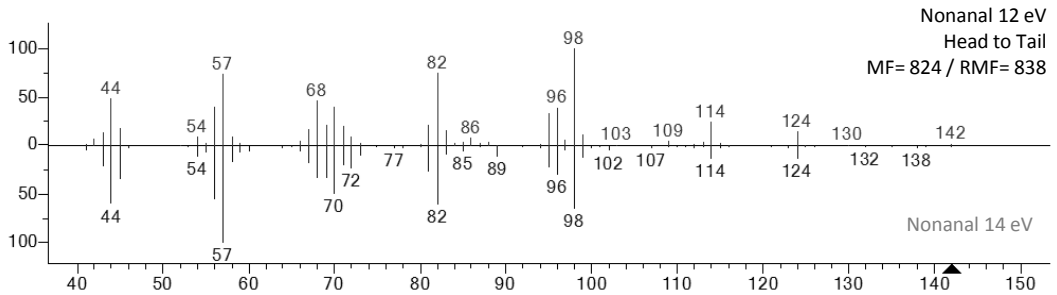
Nonanal 12 eV
Head to Tail
MF= 824 / RMF= 838
Nonanal 14 eV

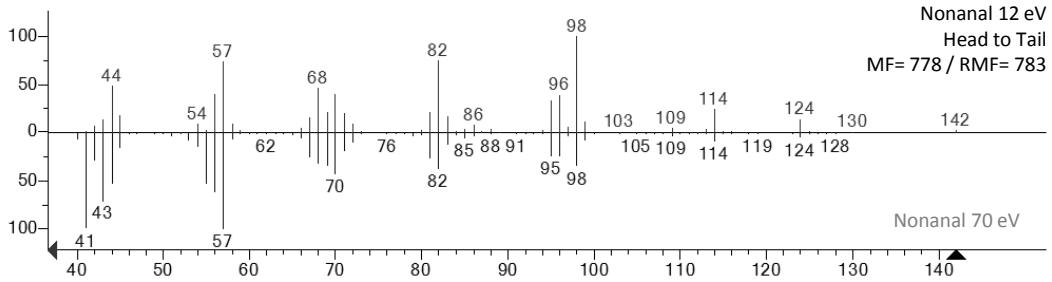
Nonanal 12 eV
Head to Tail
MF= 778 / RMF= 783
Nonanal 70 eV

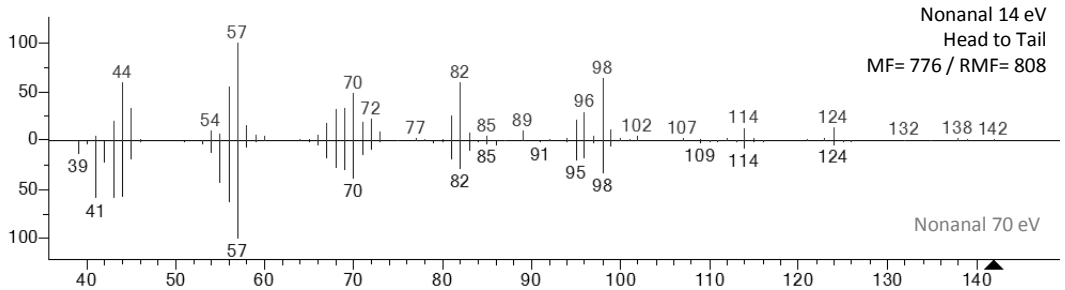
Nonanal 14 eV
Head to Tail
MF= 776 / RMF= 808
Nonanal 70 eV

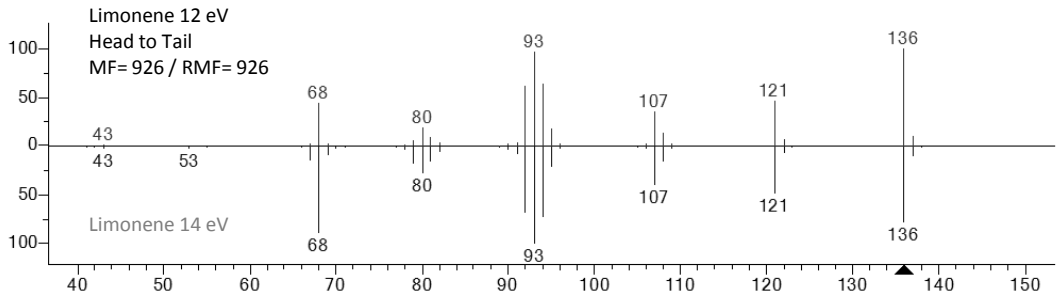
Limonene 12 eV
Head to Tail
MF= 926 / RMF= 926
Limonene 14 eV

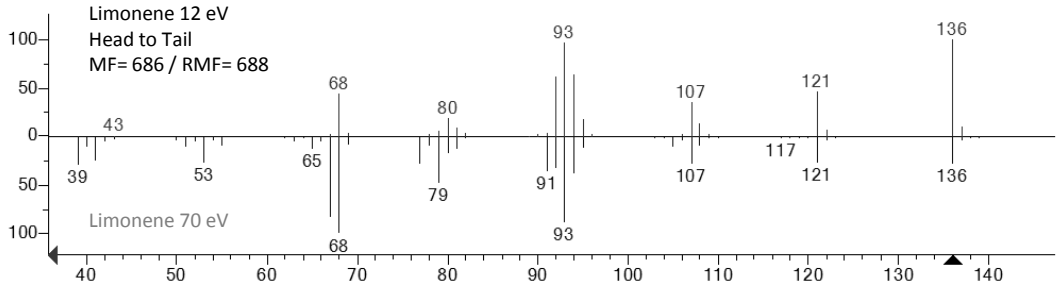
Limonene 12 eV
Head to Tail
MF= 686 / RMF= 688
Limonene 70 eV

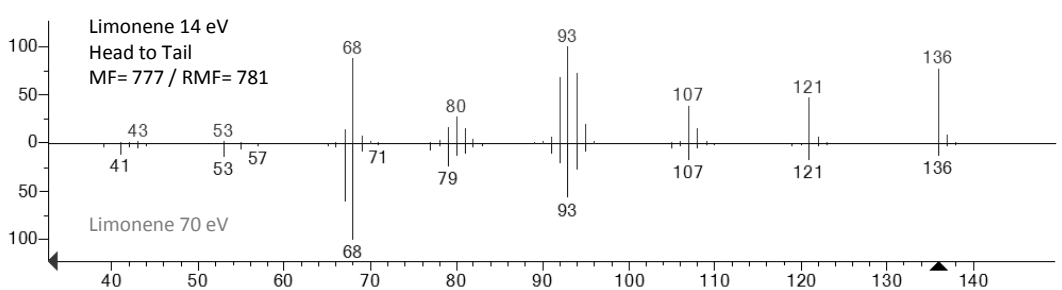
Limonene 14 eV
Head to Tail
MF= 777 / RMF= 781
Limonene 70 eV

Figure 3 color and BW

Figure 3

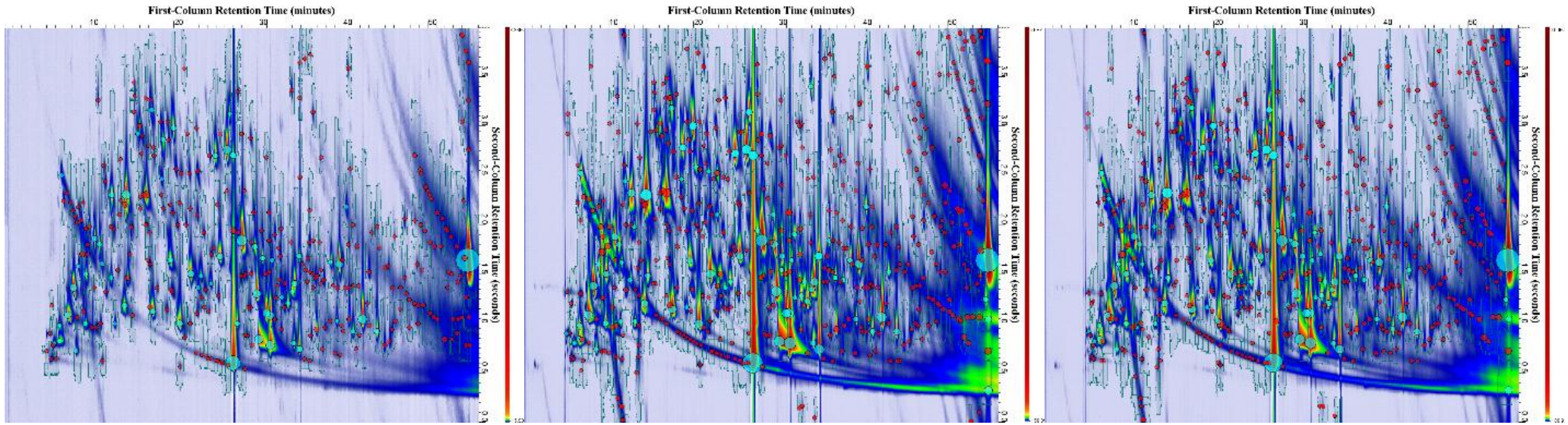

A. 12eV Composite

B. 70eV Composite

C. Summed Composite

Figure 3

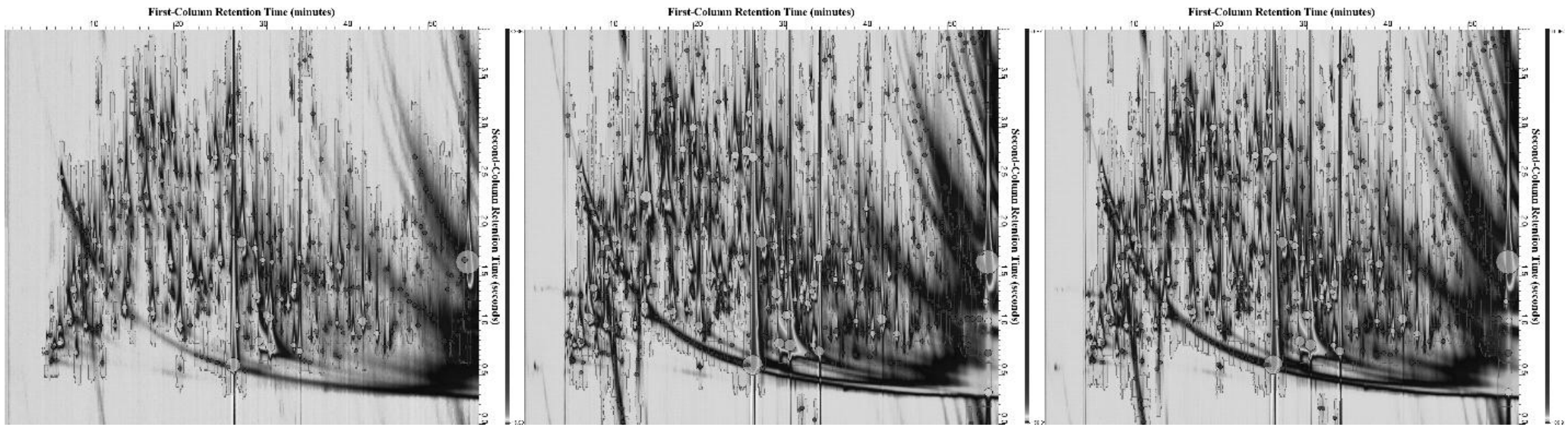

A. 12eV Composite

B. 70eV Composite

C. Summed Composite

Figure 4 color and BW

Figure 4

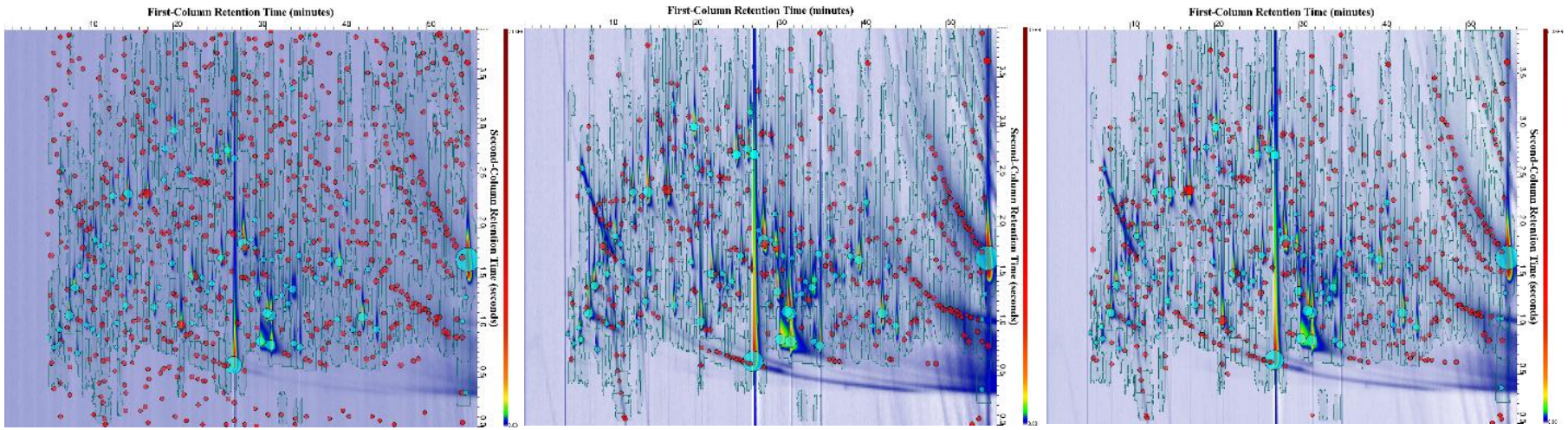

A. 12eV Chromatogram

B. 70eV Chromatogram

C. Summed Chromatogram

Figure 4

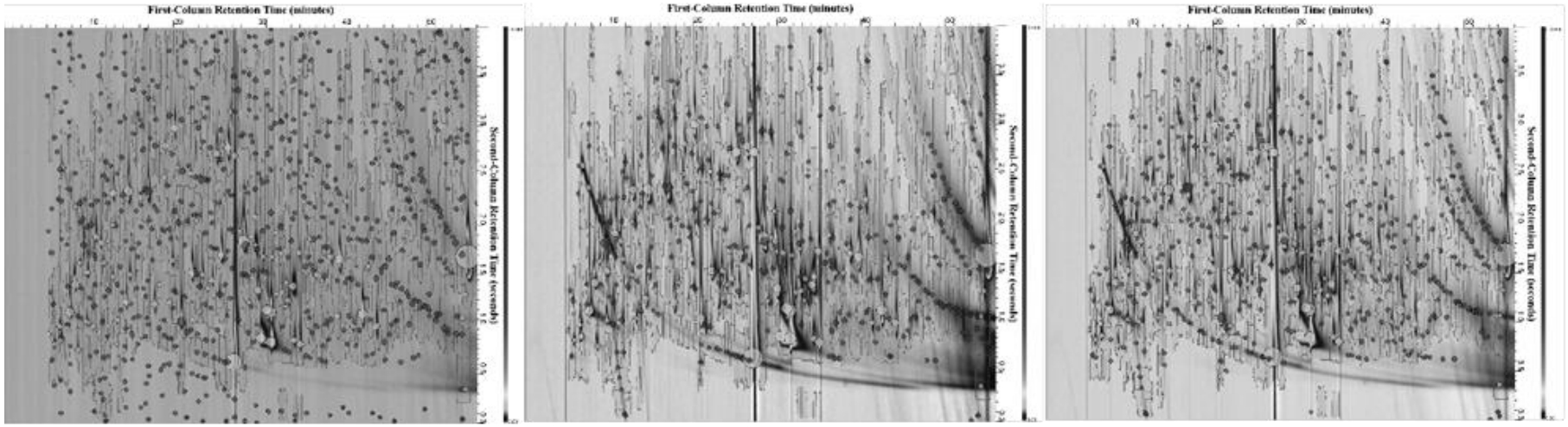

A. 12eV Chromatogram

B. 70eV Chromatogram

C. Summed Chromatogram

Figure 5 color and BW

Figure 5

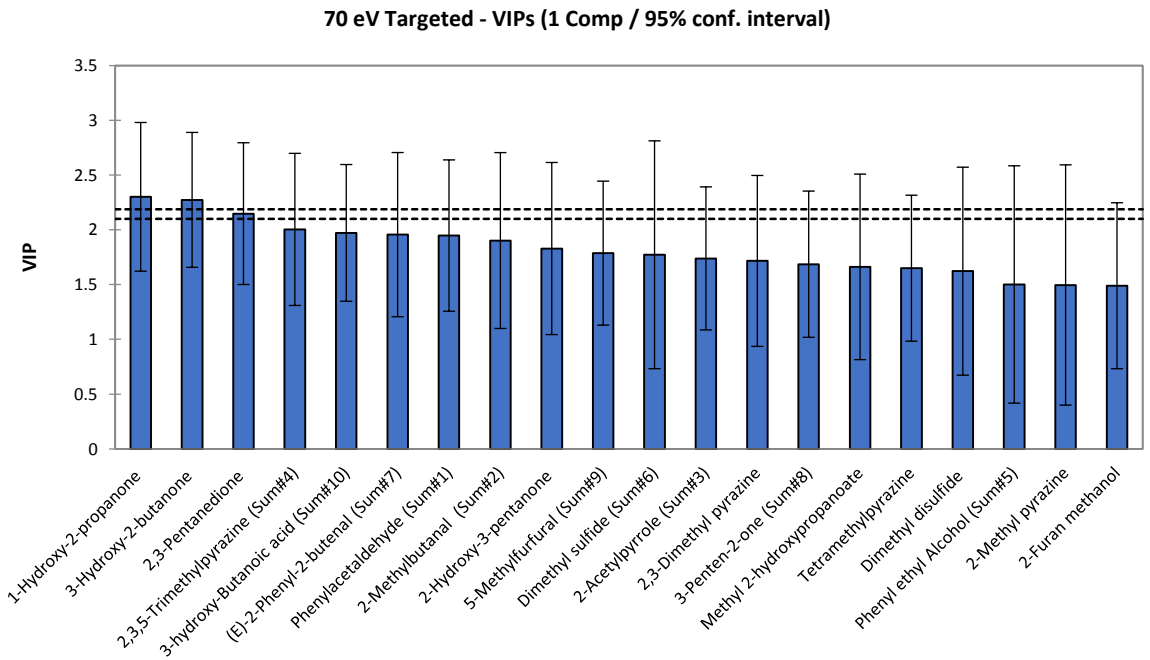

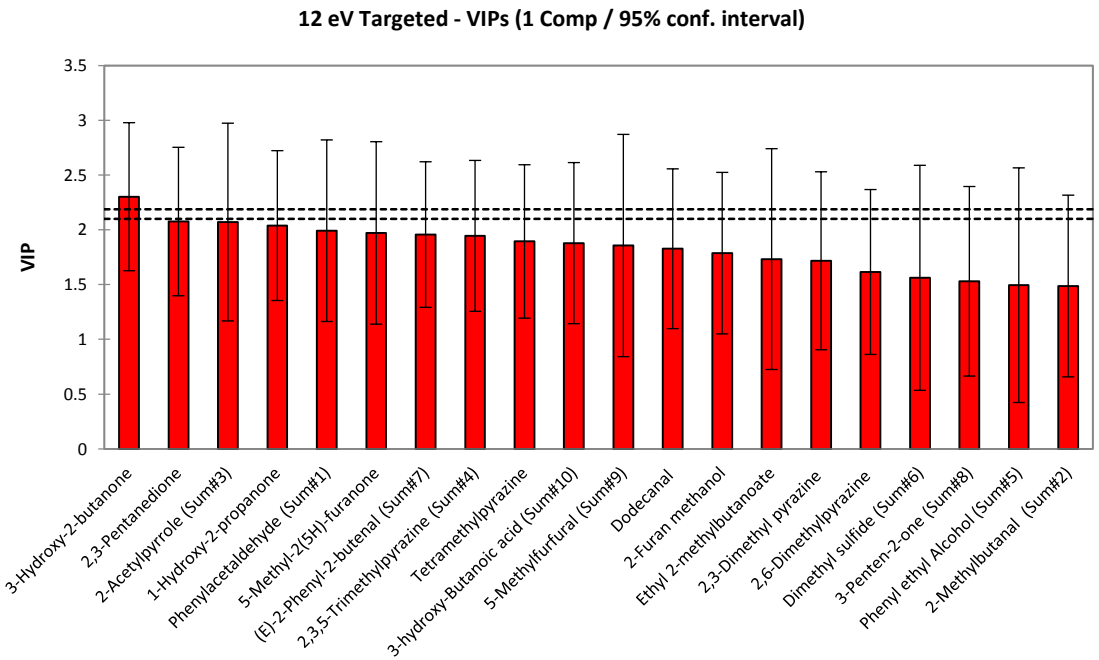

Figure 5

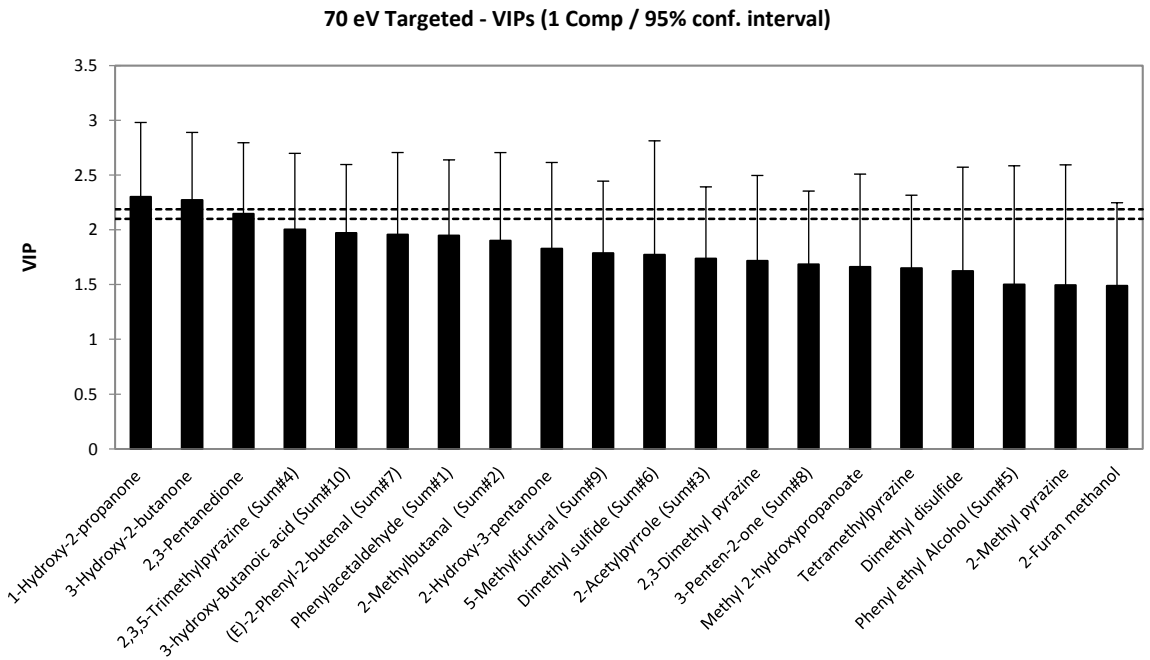
70 eV Targeted - VIPs (1 Comp / 95% conf. interval)
VIP
3.5
3
2.5
2
1.5
1
0.5
0
1-Hydroxy-2-propanone
3-Hydroxy-2-butanone
2,3-Pentanedione
2,3,5-Trimethylpyrazine (Sum#4)
3-hydroxy-Butanoic acid (Sum#10)
(E)-2-Phenyl-2-butenal (Sum#7)
Phenylacetaldehyde (Sum#1)
2-Methylbutanal (Sum#2)
2-Hydroxy-3-pentanone
5-Methylfurfural (Sum#9)
Dimethyl sulfide (Sum#6)
2-Acetylpyrrole (Sum#3)
2,3-Dimethyl pyrazine
3-Penten-2-one (Sum#8)
Methyl 2-hydroxypropanoate
Tetramethylpyrazine
Dimethyl disulfide
Phenyl ethyl Alcohol (Sum#5)
2-Methyl pyrazine
2-Furan methanol

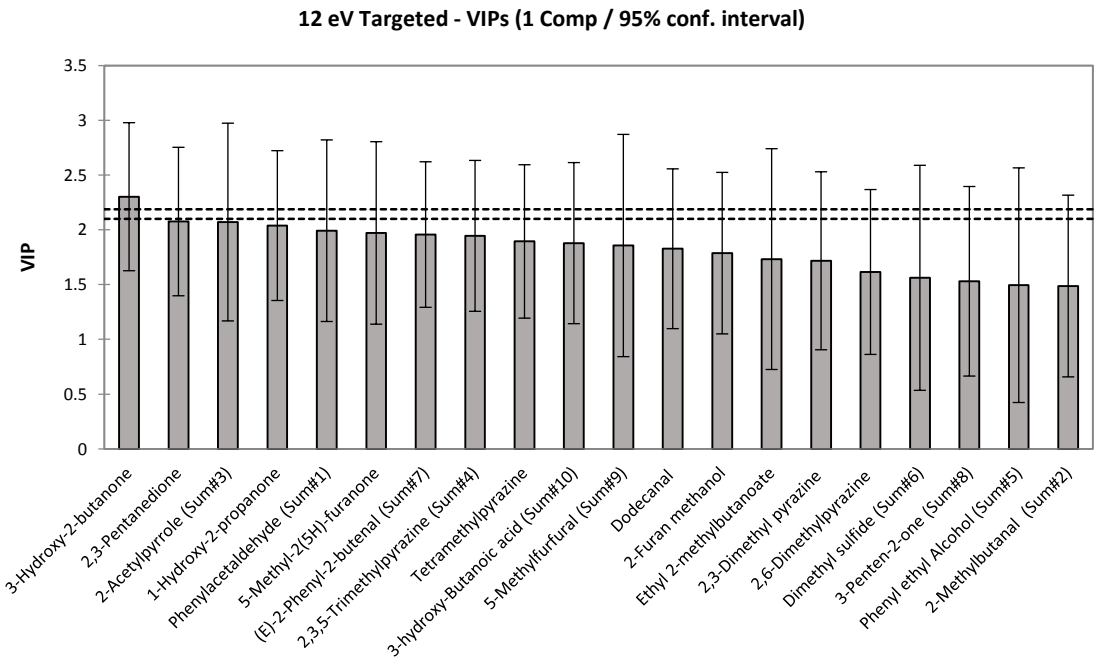
12 eV Targeted - VIPs (1 Comp / 95% conf. interval)
VIP
3.5
3
2.5
2
1.5
1
0.5
0
3-Hydroxy-2-butanone
2,3-Pentanedione
2-Acetylpyrrole (Sum#3)
1-Hydroxy-2-propanone
Phenylacetaldehyde (Sum#1)
5-Methyl-2(5H)-furanone
(E)-2-Phenyl-2-butenal (Sum#7)
2,3,5-Trimethylpyrazine (Sum#4)
Tetramethylpyrazine
3-hydroxy-Butanoic acid (Sum#10)
5-Methylfurfural (Sum#9)
Dodecanal
2-Furan methanol
Ethyl 2-methylbutanoate
2,3-Dimethyl pyrazine
2,6-Dimethylpyrazine
Dimethyl sulfide (Sum#6)
3-Penten-2-one (Sum#8)
Phenyl ethyl Alcohol (Sum#5)
2-Methylbutanal (Sum#2)

Tables

Table 1

Origin	Commercial description	Supplier - Trader	Harvest year
Mexico	*Chontalpa Cacao fermentado seco calidad Baluarte*	"Mercados alternativos y solidarios para productos del campo S. de RL. de CV" Calle Exterior Manzana 17 Lote 18 Colonia Fracc. Lomas de Ocuiltzapotlan localidad Villa de Ocuiltzapotlan referencia Tabasco Mexico http://www.lacoperacha.org.mx	2016
Colombia	Fino de Aroma Colombia Premium 1	Newchem Srl, Via M.F. Quintiliano 30 20138 Milan, Italy http://www.newchem.it	2016
Sao Tomè	Superior Cacau Fino, good fermented	Satocao LDA -Morro Peixe, Distrito de Lobata São Tomé e Príncipe - CP 762 http://www.satocao.com	2016
Ecuador	Ecuador ASS (Arriba Superior Selecto)	Domori S.r.l. - Via Pinerolo 72-74 10060 None (Torino), Italy	2016

Table 2

				70 eV *vs.* lib		12 *vs.*14 eV		12 *vs.* 70 eV		14 *vs.*70 eV		SNR		Ratio
Compound name	**^1t_R min**	**^2t_R sec**	**I^T_S**	**DMF**	**RMF**	**DMF**	**RMF**	**DMF**	**RMF**	**DMF**	**RMF**	**70 eV**	**12 eV**	**(12/70)**
3-Methyl-butanal	8.40	1.32	911	963	963	827	833	696	694	798	805	2309	4300	**1.86**
2-Methyl-butanal	8.40	1.34	911	970	981	883	902	878	909	839	868	3791	5920	**1.56**
2,3-Pentanedione	12.40	1.24	1050	973	995	914	914	810	810	817	822	512	280	0.55
Hexanal	13.33	1.82	1077	992	993	881	880	786	789	868	872	237	69	0.29
β-Pinene	14.27	3.20	1104	974	979	918	924	693	694	796	796	43	31	0.72
3-Penten-2-one	15.20	1.52	1128	983	989	850	850	682	684	835	836	765	384	0.50
Limonene	17.80	1.04	1197	985	986	926	926	717	724	773	786	277	150	0.54
Hexyl acetate	21.07	0.92	1280	982	985	922	928	737	745	911	912	529	142	0.27
Octanal	21.60	0.80	1293	990	990	848	853	805	840	793	820	50	18	0.36
Nonanal	25.60	1.16	1397	974	989	824	838	778	783	776	808	658	455	0.69
Furfural	27.93	1.78	1459	985	990	876	877	803	805	863	883	529	590	**1.12**
Benzaldehyde	30.60	0.58	1533	974	984	964	964	837	837	717	723	2296	2640	**1.15**
2(*E*)-Nonenal	30.80	1.74	1538	975	976	922	931	805	840	832	837	419	197	0.47
Linalool	31.20	1.36	1550	978	988	919	923	771	776	851	853	605	394	0.65
1-Octanol	31.67	0.62	1563	996	996	887	889	815	829	864	889	294	105	0.36
2-Furan methanol	34.60	1.30	1648	984	989	897	897	735	735	813	813	1350	2100	**1.56**
Benzyl alcohol	41.53	1.26	1862	994	995	901	901	783	787	789	789	713	450	0.63
γ-octalactone	43.33	3.04	1920	990	992	941	945	857	857	890	890	29	16	0.55
1H-Pyrrole-2-carboxaldehyde	46.13	0.84	2017	860	869	924	930	780	780	924	927	120	113	0.94
γ-Nonalactone	46.40	0.90	2026	877	978	939	949	817	817	857	862	204	95	0.47

Table 3

	70eV Composite			12eV Composite			Summed Composite		
Detected 2D-peaks in composite chromatograms with SNR ≥ 100	491			335			498		
Detected 2D-peaks in individual chromatograms with SNR ≥ 20	**70eV**			**12eV**			**Summed**		
	Run 1	**Run 2**	**Avg.**	**Run 1**	**Run 2**	**Avg.**	**Run 1**	**Run 2**	**Avg.**
Colombia Raw	456	357	407	747	811	779	497	445	471
Ecuador Raw	364	321	343	706	761	734	471	383	427
Mexico Raw	516	505	511	793	780	787	614	622	618
Sao Tome Raw	497	527	512	796	813	805	584	633	609
Average Raw		443			776			531	
Colombia Roasted	394	495	445	860	765	813	453	557	505
Ecuador Roasted	405	417	411	714	786	750	521	492	507
Mexico Roasted	470	479	475	761	761	761	510	571	541
Sao Tome Roasted	527	484	506	801	784	793	624	545	585
Average Roasted		459			779			534	

Table 4

Feature	Mean	Median	Max	Mean 10
Apex Response 12eV	0.31	0.09	6.08	3.34
Apex Response 70eV	0.40	0.17	8.12	3.74
Apex Response Sum	0.41	0.18	7.29	3.86
Volume 12eV	0.19	0.02	6.02	3.59
Volume 70eV	0.53	0.20	13.08	4.83
Volume Sum	0.53	0.18	12.16	5.30
% Resp. 12eV	0.54	0.32	6.31	3.90
% Resp. 70 eV	0.42	0.14	14.01	5.51
% Resp. Sum	0.40	0.15	12.75	5.23
Base Peak Apex Response 12eV	0.32	0.09	5.63	3.43
Base Peak Apex Response 70eV	0.38	0.16	8.83	3.96
Base Peak Apex Response Sum	0.37	0.14	8.73	3.81
Base Peak Volume 12eV	0.37	0.09	7.80	4.96
Base Peak Volume 70eV	0.42	0.14	7.52	4.37
Base Peak Volume Sum	0.41	0.13	7.77	4.41
Large-mass Apex Response 12eV	0.29	0.08	2.92	3.01
Large-mass Apex Response 70eV	0.30	0.09	5.58	3.27
Large-mass Apex Response Sum	0.30	0.08	4.95	3.07
Large-mass Volume 12eV	0.34	0.08	6.31	3.87
Large-mass Volume 70eV	0.34	0.08	6.42	4.00
Large-mass Volume Sum	0.35	0.08	6.31	4.42

Table 5

			Significance Rank		
Area ID	**Compound name**	**^1t_R min - ^2t_R sec**	**Sum**	**70eV**	**12eV**
37	Phenylacetaldehyde	(33.98, 1.33)	1	1	2
14	2-Methylbutanal	(8.18, 1.36)	2	2	1
38	2-Acetylpyrrole	(43.99, 0.91)	3	3	4
26	2,3,5-Trimethylpyrazine	(25.43, 1.68)	4	4	6
4	Phenyl ethyl alcohol	(42.28, 1.05)	5	5	3
134	Dimethyl sulfide	(6.08, 2.80)	6	7	5
68	(E)-2-Phenyl-2-butenal	(43.03, 1.53)	7	6	138
52	3-Penten-2-one	(14.60, 1.52)	8	11	10
86	5-Methylfurfural	(31.58, 1.64)	9	9	29
102	3-hydroxy-Butanoic acid	(32.03, 1.25)	10	8	177